Study of variations of the carrier recombination and charge transport parameters during proton irradiation of silicon pin diode structures

E. Gaubas, T. Čeponis, J. Vaitkus, and J. Raisanen

Citation: AIP Advances **1**, 022143 (2011); doi: 10.1063/1.3605715

View online: http://dx.doi.org/10.1063/1.3605715

View Table of Contents: http://scitation.aip.org/content/aip/journal/adva/1/2?ver=pdfcov

Published by the AIP Publishing

Study of variations of the carrier recombination and charge transport parameters during proton irradiation of silicon pin diode structures

E. Gaubas,[1,a] T. Čeponis,[1] J. Vaitkus,[1] and J. Raisanen[2]
[1]*Institute of Applied Research, Vilnius University, Lithuania*
[2]*Division of Materials Physics, Department of Physics, University of Helsinki, Finland*

(Received 25 March 2011; accepted 13 May 2011; published online 20 June 2011)

Techniques for the remote and in situ control of carrier recombination and drift parameters during proton irradiation are presented. The measurement and evaluation of the carrier recombination and drift-diffusion characteristics are based on simultaneous analysis of microwave probed photoconductivity transients and of the induced charge collection current transients in diodes with applied electric field during the proton exposure. *Copyright 2011 Author(s). This article is distributed under a Creative Commons Attribution 3.0 Unported License*. [doi:10.1063/1.3605715]

I. INTRODUCTION

Evaluation of the mechanisms of radiation damage of particle detectors in the range of high fluences is commonly implemented by combining of several techniques. Examination of leakage current, of carrier generation lifetime is performed by thermal stimulated current (TSC),[1] by capacitance deep level transient spectroscopy (DLTS),[2,3] and by exploiting measurements of drift current transients (TCT),[4,5] in analysis of the post-irradiation state of devices.

However, capacitance and depletion based measurements (DLTS, C-V and TCT) become complicated when high resistivity material (with rather small doping density) is exploited in fabrication of particle detectors. Then, heavily irradiated diodes may experience a transition to an insulating substance state with rather small free carrier concentration (due to high density of different type carrier capture centers) insufficient to sustain a depletion boundary, by exhibiting a long dielectric relaxation time. Therefore, evaluation of carrier capture and generation lifetimes as well as other important parameters becomes complicated when depletion width based techniques are employed. Although, concerted analysis and the deduced characteristics in lightly irradiated structures might be useful to anticipate trends and primary understanding of the radiation induced defect complexes and their impact on functional characteristics of particle detectors.[6] However, in the range of high irradiation fluences ($\Phi > 10^{14}$ cm^{-2}), application of the above-mentioned techniques is complicated since the radiation defect density significantly overpasses the concentration of dopants, and cluster formation may become the dominant mechanism in radiation damage of the detector material. Additionally, measurements carried out after the irradiation do not provide direct information on the evolution and interactions within the densely radiation damaged material. Peculiarities in extracting of the carrier recombination and trapping parameters from the microwave probed photoconductivity transients (MW-PC) measured in situ during protons irradiation in wafer samples without applied electric field are presented in 7.

In this work, techniques (the instrumentation, the combined measurement regimes and the modified methods) for the in situ control of the carrier recombination and transport parameters, during irradiation by protons of 8 MeV energy, are presented. Simultaneous measurements of the microwave probed photoconductivity transients by using different bias voltages and excitation

[a]Corresponding author: eugenijus.gaubas@ff.vu.lt

wavelengths combined with induced charge diode current (ICDC) and induced charge collection current (IChCC) transients implemented in parallel and perpendicular excitation regimes are described. The regimes for control of detector parameters during proton exposure by the combined use of transient methods and dc leakage current control implemented via the remote measurement arrangements are discussed. It has been demonstrated that the evolution of radiation defects and changes of the carrier recombination-transport parameters during irradiation can be deduced by the combined monitoring of the above-mentioned transient and dc characteristics.

II. INSTRUMENTATION FOR THE REMOTE CONTROL OF CARRIER RECOMBINATION/TRANSPORT CHARACTERISTICS

The transient current technique (TCT) is widely employed[4,5] in characterization of the irradiated detectors by exploiting rather high sensitivity (existence of a response at rather low excess carrier densities) of this method and its ability to separate the carrier drift parameters for electrons and holes. However, the excess carrier capture/recombination parameters are extracted indirectly from the measured TCT transients[4] by using a procedure for the re-constructing of the shape and amplitude of the measured TCT signal.[5] The last procedure, made only by analysis of the integral over TCT pulse duration,[5] is non-well-defined when an excess carrier generation term is ignored, especially for short carrier capture times. The main difficulty appears, when applying this technique for heavily irradiated diodes, due to increment of dielectric relaxation time, which can become significantly longer than carrier capture/emission lifetimes. Then, the procedure for re-constructing of the shape and amplitude of the measured TCT signal is furthermore complicated, due to indefinite depletion boundary and induced charge domain widths. Then, the electric field distribution uncertainty with inherent double peak transient shape and its impact on the carrier capture parameters is a complicated problem. In the heavily irradiated detectors, extraction of the drift-recombination characteristics becomes more complex when carrier lifetime is shorter or close to carrier drift duration. Thus, carrier diffusion and recombination processes might be a reason for complicated modifications of TCT transients, including the discussed above reasons, as well. Therefore, various regimes of simultaneous measurements of the induced charge diode current (ICDC) and induced charge collection current (IChCC) transients combined with microwave contact-less probed photoconductivity transients measured with applied electric field (MW-PC-E) have been employed for an in situ examination of the 8 MeV protons radiation induced changes of material parameters in the particle pad-detector structures. Measurements were carried out at T=300 K.

The experimental arrangement for the remote measurements of the microwave probed photoconductivity (MW-PC-E) and ICDC/IChCC signals is designed on the basis of the MW-PCT instrument described in 7. The additional components and biasing circuitry, installed within this MW-PC-E instrument, are sketched in FIG. 1. Several experimental geometries of excitation – signal recording have been exploited, namely: i) a perpendicular excitation regime is performed by combining excitation and MW-PC probes linked at the diode boundary while ICDC and IChC current directed parallel to the ion beam is recorded synchronously; ii) excitation fiber-tip is positioned on a rear side of a diode in parallel to proton beam direction, while MW needle-tip probe is located on diode boundary; iii) the parallel positioning of the MW-PC needle-tip and of excitation fiber tip through a non-metallized diode window is also possible. A light wavelength of 1062 nm is used for bulk excitation while radiation of a second harmonic at 531 nm of the same microchip pulsed (400 ps) laser is employed for generation of a surface domain of the excess carriers. The proton beam induced current is continuously controlled by measuring the total leakage current in a reversely biased pin diode under investigation. The transient MW-PC-E and ICDC/IChCC signals are synchronously registered on different channels of oscilloscope while the bias and proton beam induced dc voltage components are rejected by capacitors installed at oscilloscope inputs. The recorded signals are transferred outside the accelerator control area and measured by a 1 GHz Tektronix oscilloscope TDS-5104. An oscilloscope screen image of the simultaneously registered transients is illustrated in the inset of FIG. 1.

During the initial irradiation stages, a proton beam current has been kept rather small (of about 0.5 nA) to decrease noises within ICDC signals and to avoid excess carrier induced the

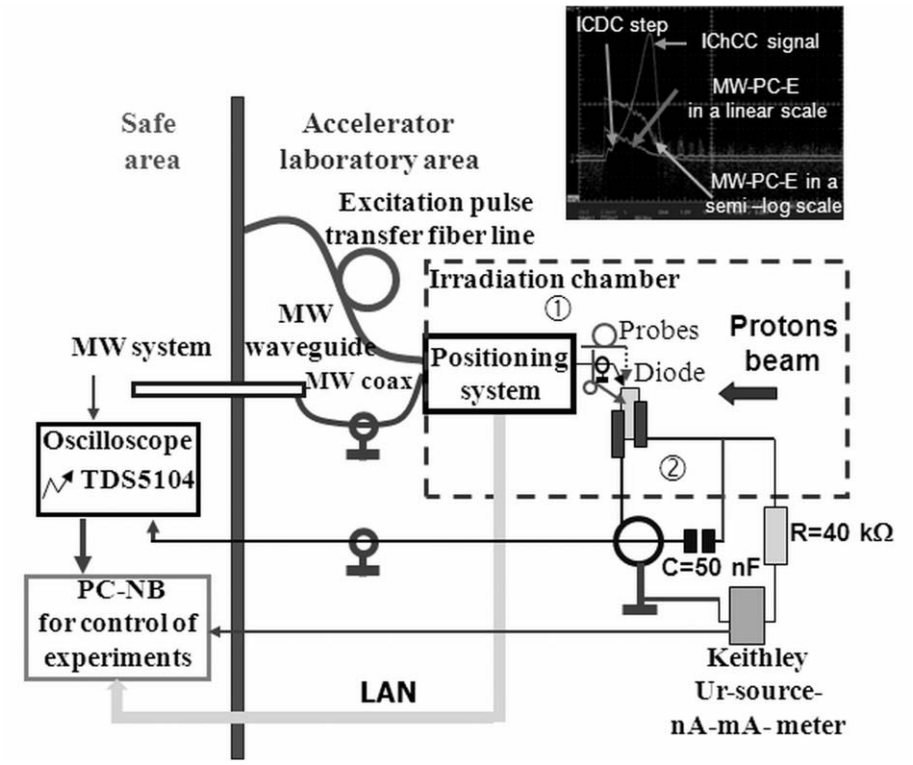

FIG. 1. Sketch of the setup for the simultaneous measurements of carrier transport and recombination characteristics under applied bias electric field during irradiation by protons beam: 1- excitation fiber-tip and MW needle–tip probes for contact-less measurements of the photoconductivity (MW-PC-E) transients, 2- a circuitry for electrical biasing and ICDC/IChCC transients registration inside vacuumated irradiation chamber. In the inset, an oscilloscope screen image of MW-PC-E and ICDC/IChCC transients simultaneously recorded by Tektronix oscilloscope TDS-5104.

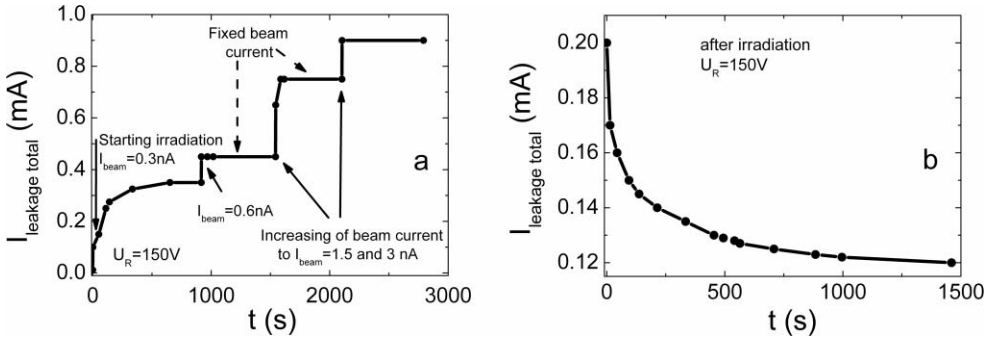

FIG. 2. a- Diode leakage current as a function of irradiation time. The steps correspond to increase of the proton flux. b – Leakage current relaxation due to radio-nuclide decay just after proton beam is switched-off.

impact ionization avalanche breakdown effect, inherent for the elevated proton fluxes.[8] During the irradiations also the beam current (i.e. flux) was altered to measure more precisely variations of the carrier recombination/transport parameters within the diode base material ascribed to different exposure instants. Corresponding clear steps of leakage current increase were resulted, as seen in FIG. 2(a). These changes appear due to excess carrier generation by protons,[8,9] and due to enhanced thermal emission from radiation induced carrier traps.

Control of the total leakage current is also useful for estimating the impact of radio-isotopes produced by nuclear reactions during the proton bombardment. The impact can be deduced by measuring the relaxation characteristic of leakage current (FIG. 2(b)) either in between of beam

current change steps or just after switching off the protons beam. However, neither the proton irradiation (at beam area 0.3 cm^2 and beam current <20 nA) flux of $<4\times10^{11}$ protons/cm^2s induced steady-state excess carrier densities $<10^6$ $cm^{-3}s^{-1}$ nor those generated by decaying radio nuclides approach the generation rate obtained by the short laser pulses (of the order of $>10^{27}$ $cm^{-3}s^{-1}$) exploited in the photo-excitation of the MW-PC-E and ICDC/IChCC transients. Therefore, the MW-PC-E and ICDC/IChCC transient techniques can be valuable tools for in situ monitoring of defect creation even when the particle fluxes are considerably higher.

III. SAMPLES

Particle pad-detectors[10] fabricated either from n- or p- type CZ (Czochralski grown) Si supplied by Okmetic Ltd were used for the MW-PC-E and ICDC/IChCC transient studies. The detectors were processed at the Microelectronics Centre of Aalto University, Finland. The detectors with (p^+-n-n^+) diode structure had an active area of 5 × 5 mm^2 which was surrounded by 16 floating guard rings. A more detailed description of the detector structure is provided in 11. The diode base material has resistivity of about 1100-1200 Ωcm (with equilibrium majority carrier density of about (2-4)× 10^{12} cm^{-3}) and base thickness 280-300 μm. The full depletion voltage of the non-irradiated base is of about 130 V (while a breakdown voltage is >9 kV). Additionally, the pad-detectors contain a non-metallized hole of a diameter of ∼ 1 mm within a centre of the main junction electrode for light excitation.[10]

A special sample holder (FIG. 3) was fabricated to enable proper electrodes for the electrical circuitry and windows as diaphragm for the proton beam and optical excitation. A freshly cleaved cross-sectional boundary of a pad-detector broken into halves was used for a perpendicular bulk excitation and MW-PC-E probing by the coaxial needle-tip MW antenna (components marked by ① in FIG. 1) with several measurement geometries. In the case of parallel excitation geometry, a MW-PC-E photo-response was registered by a positioned needle-tip MW antenna either on the pad-detector boundary (using a 3D stepper motor driven stage containing a flexible bellow) or on a non-metallized hole/smash rear electrode. It has been earlier verified[7] that no significant impact is induced on the MW-PC-E probes by the protons (within the energy range of 2 - 9 MeV and a beam current in the range of 0.5- 20 nA).

IV. RESULTS AND ANALYSIS OF THE IN SITU VARIATIONS OF CARRIER TRANSPORT-RECOMBINATION CHARACTERISTICS

A. Examination of ICDC transients by using the lowest excitation density

Variations of the injected charge induced diode current (ICDC) transients at excitation densities necessary to obtain signal just above ICDC noise level have been measured by using either the surface (531 nm excitation wavelength) or bulk (1062 nm wavelength) excitation regimes with laser pulses of about 10^2 fJ per 400 ps, by lighting either a non-metallized hole (531 nm) on the diode or using a perpendicular geometry (1062 nm) when laser beam impinges on the region of junction. In this case, the excitation density is below the threshold of resolving the MW-PC response. The ICDC signals were registered at applied voltages above the full depletion voltage ($U>U_{FD}$) of non-irradiated diodes. The ICDC transients registered in situ at different 8 MeV proton exposure instants are illustrated in FIG. 4(a) for the photo-injected surface (531 nm) charge domain of electrons within n-base. The shape and duration of ICDC pulses appear to be approximately invariable with enhancement of irradiation time.

In order to understand nearly independent shape and duration of ICDC transients and to validate procedures of the extraction of material parameters, formation of the injected charge induced diode current (ICDC) transients are considered in more detail. A sketch of the electric field distribution within the n-base of a diode under injected excess carrier pairs ($n_{ex}=p_{ex}$) is shown in FIG. 5. For applied voltages $U<U_{FD}$, the current in the external circuit flows due to simultaneous extraction of the majority equilibrium carriers (n_0, p_0) from the electrically neutral n-base and p^+ regions caused by separation (due to steady-state field) of the injected excess carrier pairs (and extraction of excess

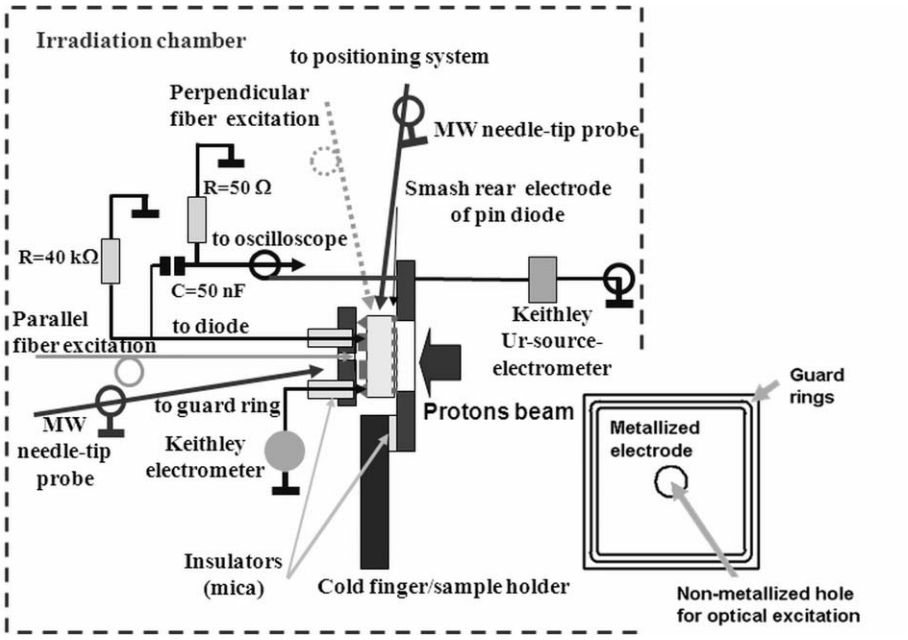

FIG. 3. Pin diode attachment to the sample holder inside the vacuum chamber for combined MW-PC-E and ICDC/IChCC transient measurements. In the inset the front side of the pad-detector is illustrated.

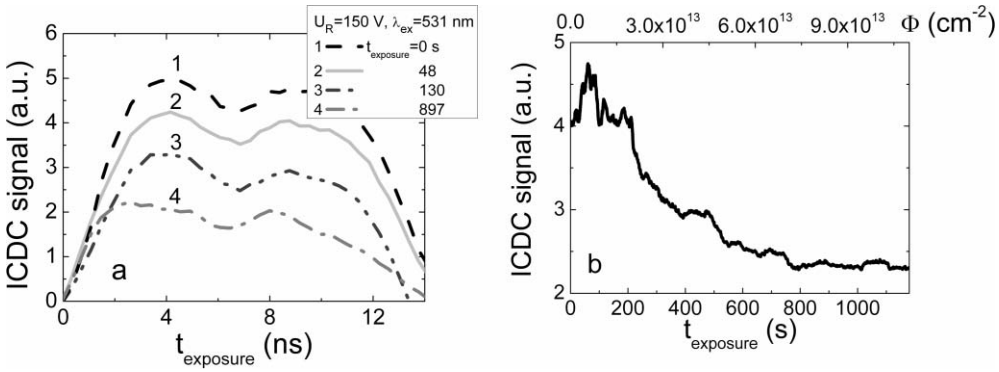

FIG. 4. a- Variations of the ICDC transients; b- ICDC pulse amplitude as a function of exposure time to 8 MeV protons, measured by using the regime of the surface excitation (531 nm) of excess carriers at fixed bias voltage $U \geq U_{FD}$.

holes from the n-base region into the p^+ region). During this process, the first peak within ICDC transient appears.

The separation process induces the change of depletion width $w_{q,n}$ (relatively to its steady-state value w_0) due to surface field domain $-q_e/\varepsilon_0\varepsilon$ of excess electrons. The extracted excess holes are located at p^+-side producing the same value of surface field. Thus, the overall charge balance ($w_{q,p+}N^-_{A,p+}=w_{q,n}\,N^+_{D,n}$) in diode is maintained. This balance in n-base is supported by applied dc voltage (U) together with a surface charge $q_h/\varepsilon_0\varepsilon$ (in p^+layer), if q_e domain separated at length $X_{0,n}$ (from metallurgic boundary) exists within a depleted region w_0 of n-base. Then for $U<U_{FD}$, using a depletion approximation, standard in device physics,[12,13] the electric field $E(0)$ at the metallurgic boundary ($E(0)=[(2eN_D/\varepsilon_0\varepsilon)\{U+(q_e/\varepsilon_0\varepsilon)X_0)\}]^{1/2}- q_e/\varepsilon_0\varepsilon$) and depletion width

$$w_q = \sqrt{\frac{2\varepsilon\varepsilon_0 U}{eN_D} + \frac{q_e}{\varepsilon\varepsilon_0}X_0} \qquad (1)$$

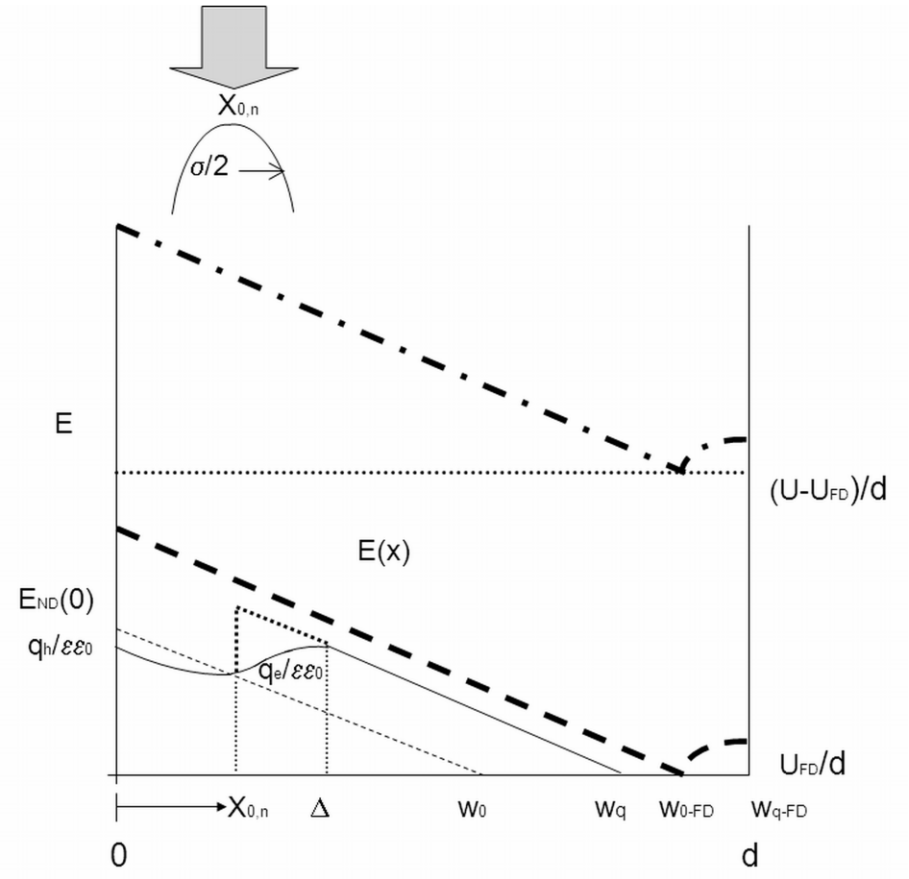

FIG. 5. A sketch of electric field distribution due to induced surface charge for different applied dc voltage values: $U<U_{FD}$ – dot and solid lines, $U\cong U_{FD}$ and $w_q=d$ – dash line, $U>U_{FD}$ dash-dot line. For $U<U_{FD}$, the enlarged details of field distribution are shown, where dot line is attributed to an induced surface-charge field $q_e/\varepsilon\varepsilon_0$, while the solid line represents an excess carrier charge domain of width Δ.

(due to q_e with separation length X_{0n}) is evaluated. The electric field distribution is sketched in FIG.5 by a dot-line, for a surface charge q_e separated at length $X_{0.}$ Here, depletion width (w_0, w_q) trivially means that material is electrically neutral (the potential together with electric field are zero) at this point.[12] The ICDC flows during $q_e(t)$ relaxation (due to capture of excess electrons within the depleted n-base region by deep centers) and changing of a separation length $X_{0n}(t)$ (e.g., due to capture of excess holes in depleted p^+ region), till w_q recovers to w_0. The latter relaxation process is clearly non-exponential, and it is described by the solution of a transcendental equation

$$q_e(t) = eN_D\sqrt{\frac{2\varepsilon\varepsilon_0 U}{eN_D} + \frac{q_e(t)}{\varepsilon\varepsilon_0}X_0(t)} - \frac{eN_D X_0(t)}{1-\exp(-t/\tau_M)}. \quad (2)$$

Here, $\tau_M = \varepsilon_0\varepsilon/eN_D\mu_e$ is a dielectric relaxation time, e - elementary charge, ε_0 and ε are vacuum and material permittivity, respectively, $N_D = n_0$ is an effective doping density. Infinitely narrow, sketched by a dot-line in FIG.5, injected surface-charge is an idealization.

Actually, a close to Gaussian profile of excess carrier density is induced by a 1062 nm light laser beam when using a perpendicular (to current direction) excitation geometry. Thus, the excess carrier domain induced surface field can be found by combining integrals of Gauss and of Poison equation, and it can be evaluated as

$$E_s \cong en_{ex0}\bar{\sigma}(\pi/2)^{1/2}[1+\mathrm{erf}\{(\Delta - X_0)/\bar{\sigma}(2)^{1/2}\}]/\varepsilon_0\varepsilon. \quad (3)$$

Here, σ is a width of Gaussian beam, n_{ex0} is the excess carrier density photo-generated at a base layer surface, Δ is an effective width of the light injected charge domain. The latter should be taken as $\Delta \cong 3\sigma$ if the averaged carrier density is to be controlled with high precision relatively to n_{ex0}. The solid line in FIG.5 shows the electric field distribution including the outspread of injected surface charge domain. More complicated evaluation of the generation of the surface field domain appears for parallel excitation regime. However, it can be estimated as $E_{s,p} \cong en_{ex0}\alpha^{-1}[1- \exp(-\alpha\Delta_p)]/\varepsilon_0\varepsilon$. Here, α is a light absorption coefficient at excitation wavelength, $\Delta_{p=}5\alpha^{-1}$ is an effective width of the light injected charge domain for parallel excitation regime, when the averaged carrier density is to be controlled with precision of 1% relatively to n_{ex0}. The outspread of injected surface charge domain (for both the perpendicular and parallel excitation regimes) is the main reason in formation of the double peak shape of a ICDC pulse, if applied voltages value approaches to that of U_{FD} ($U \geq U_{FD}$).

Then, the first peak in ICDC signal is again associated with excess hole extraction into p^+ layer and simultaneous majority (p_0) hole extraction from electrically neutral p^+ (with w_{p+} increment) layer towards metallic electrode and the external circuit. The second peak within ICDC transient appears due to $w_q=d=w_{q,FD}$ at full depletion, with d a geometrical thickness of the n-base layer. At full depletion (U_{FD}) voltage, the steady-state electric field is zero at $x_{FD}= w_{q,FD} - w_{0,FD}$. Thus, the last stage of excess carrier extraction runs within increasing field region, i.e. the self-acceleration of excess electrons appears to extract the excess carrier domain into the external (relatively to a base region) electrode (n^+ layer). The similar (but opposite) effect appears in extraction of excess holes from n-base, - the extracted and localized at p^+ layer ($X_{0,p+} \cong (N_{D,n}/N_{A,p+})X_{0,n}$, if carrier capture by deep traps during separation of excess holes and electrons can be ignored), these holes reduce the steady-state field at $x=0$ and slow down the later their extraction process. Therefore the ICDC initial peak is smoothed. The inherent for ICDC double peak transients are observed in FIG. 4(a). As discussed above, a rather corrugate electric field distribution appears for applied voltages $U \leq U_{FD}$. An enhancement of U above U_{FD} leads to the approximately uniform field (at $U > U_{FD}$) distribution through the base of a pin diode, and electric field is supported by planes of charge located at the external (layers) contacts.

The smoothing of the field at $U > U_{FD}$ enables one to simplify evaluation of the mobility of excess carriers by using a well-known[14] relation $\mu_e = d^2/\tau_{tr}U$ and drift time τ_{tr} measurements within ICDC pulse. To evaluate changes of material during irradiation, measurements of carrier mobility at excess carrier densities $n_{ex} < n_{0,}$ close to that values in dark are preferential, therefore the least possible excitation densities were kept in our μ_e measurements. Commonly a drift time is evaluated as a time interval for time of flight (TOF) pulse (at $U > U_{FD}$, when $\tau_{tr} < \tau_M$), however, in our case initial delay within the rise to peak appears due to several reasons: through excess carrier temporal variations during laser pulse (τ_L) and through $RC \approx 0.6$ ns of the measurement circuitry. Actually, the rise to peak duration τ_f should be taken of $\tau_f = 5RC$ to increase precision. Value of $\tau_f = 2.5$-3 ns is really obtained (FIG. 4(a)). Therefore the more reliable way to extract τ_{tr} is estimation of the time interval between the ICDC peaks, those really indicate the steadied excess carrier generation and separation process. The extracted values of electrons mobility $\mu_e = d^2/\tau_{tr}U \cong 1300$ cm^2/Vs (for non-irradiated sample) validate the chosen interval for drift time measurement. The determined mobility value variations $\Delta\mu/\mu < 20\%$ (estimated from the dispersion of τ_{tr} values during irradiation) show a small impact of irradiation on the carrier scattering parameters. It is in quantitative agreement with results published in 15.

The ICD current, associated with injected excess electron charge domain, for $U \leq U_{FD}$, varies due to temporal changes in $w_q(t)$. As $w_q(t)$ contains a product of the induced charge relaxation $q(t)$ and of pair separation length $X_0(t)$ parameters, generally the ICD current is composed of two components. Using depletion approximation, this i_{ICD} current is obtained as

$$i_{ICD}(t) = \frac{C(t)U}{\tau_M}\frac{C(t)}{C^*}\left(\frac{q_e(t)/eN_D}{w_q(t)} - 1\right) + \frac{C(t)U}{\tau_{capt}}2\frac{n_{ex}}{N_D}\frac{X_0(t)}{w_q(t)}. \quad (4)$$

Here additional symbols represent: $C(t)=\varepsilon_0\varepsilon S/w_q(t)$, $C^*=\varepsilon_0\varepsilon S/[q(t)/eN_D]$, τ_{capt} is carrier capture lifetime within depleted region, S is area of a junction. The first constituent in expression of $i_{ICD}(t)$ represents variations of separation length (for $dX_0/dt \neq 0$) while the second one is ascribed to excess

electrons capture process (for $dq/dt=edn_{ex}/dt= -en_{ex}/\tau_{capt}$) within the depleted n-base region. It can be deduced, that an enhancement of excess carrier density (of the n_{ex}/N_D) would be preferential to clarify the excess electrons trapping processes over excess holes trapping in p^+ depleted layer.

A reduction of the ICDC signal amplitudes in FIG. 4 implies shortening of the excess carrier lifetime. This result is in agreement with a characteristic evaluated directly from excess carrier decay transients in the same material.[16]

The presented in FIG. 4 characteristics enable one to estimate variations of the excess carrier drift and trapping parameters. However, enhancement of precision for extraction of parameters on high resistivity material is limited by a long Debye length ($5L_D \geq 40$ μm for Si of 1 kΩcm) in evaluation of steady-state depletion width and by a finite width of the injected excess carrier domain ($\Delta > 6$ μm for excitation wavelength of 531 nm and $\Delta > 80$ μm for red light). These widths also limit precision in evaluation of the depletion voltage values.

B. Analysis of carrier recombination/transport characteristics by using induced charge collection and photoconductivity transients

The elevated excitation ($n_{ex/N_D} \rightarrow 1$) regimes have been involved to highlight carrier recombination – diffusion processes and in order to directly control changes of the parameters of these processes. Actually, carrier capture rate within the electrically neutral region of the diode base determines the operational features of a diode when density of radiation defects increases (and may significantly exceed n_0) with irradiation fluence.

1. Examination of correlated variations of the MW-PC-E and IChCC transients

There appear a few peculiarities within simultaneously recorded microwave probed photoconductivity transient at applied electric field (MW-PC-E) and for induced charge collection current (IChCC) transients, illustrated within the inset of FIG.1 and in FIG. 6 (IChCC). The latter FIG.6 shows changes of IChCC transients by varying bias voltage (FIG. 6(a)) and excitation density (FIG.6(b)). It can be also noticed in FIG. 6(b) that both the amplitude of the second peak within a IChCC transient and duration of a IChCC pulse increase with excitation density. It can be deduced that the IChCC transient becomes shorter, and its shape approaches the double peak constitution when the applied voltage increases above full depletion voltage for non-irradiated diode, as illustrated in FIG. 6(a) for IChCC transients registered at a fixed surface excitation density. Only voltages close to U_{FD} value were appropriate in MW-PC-E measurements. An enhancement of applied voltage above U_{FD} leads to the crucial instabilities within MW-PC-E transients and to an abrupt increase of current within IChCC response, when excess carrier density n_{ex} approaches to or exceeds values of doping n_0 one (especially for bulk excitation regime). This effect can be easily understood as an evolution of the impact ionization processes (which might be mediated by Pool-Frenkel effect), when elevated density of carrier plasma crucially distorts the MW response. The registered transients (FIG. 6) imply a considerable impact of the ambipolar diffusion-recombination in the case of enhanced excitation densities, when excess electrons are collected at n^+ electrode (which blocks holes), and a current of collected charge flows within external circuit, with consequent IChCC signal detection on 50Ω load resistor. This can be applied for a direct estimation of a reduction of carrier lifetime and of diffusion length during irradiation.

The models of space charge limited current (SCLC) transients[14] are formulated for the large externally injected charge $Q > CU$, but at assumption of a negligible carrier diffusion. Then, a peak of current density is predicted at time instant of $t_1 \cong 0.78\tau_{tr}$, and current density during time instants $t_i < t_1$ is expressed as $j(t_i)=(\varepsilon\varepsilon_0\mu U^2/2d^3)(1-t_i/2\tau_{tr})^{-2}$. However, description of the backward constituent of the SCLC transients is much more complicated for arbitrary injected charge, and only a numerical simulation of transient parameters is possible in the general case.

To qualitatively simulate the experimentally observed transients of the induced charge collection current (IChCC) and photo-conductivity transients probed by microwaves (MW-PC-E) (inset of FIG.1), a simplified model has been employed in this work.

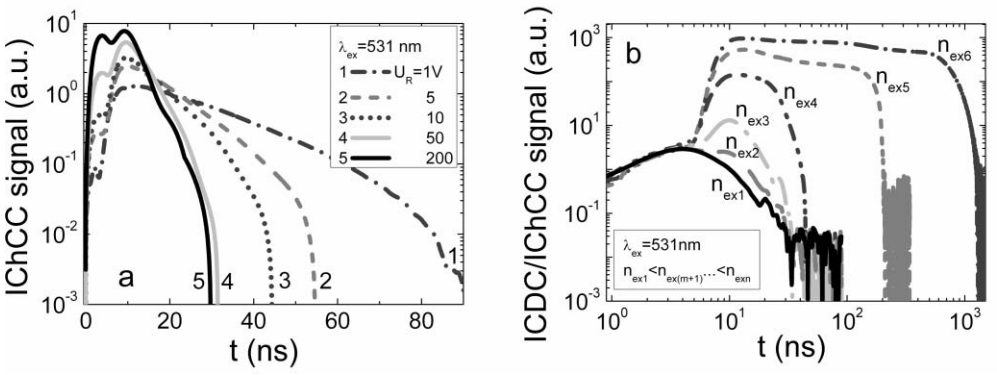

FIG. 6. Variation of the ICDC/IChCC transients as a function of applied voltage at fixed excitation density (a) and of excitation density at fixed bias voltage (b) measured on a non-irradiated Si diode.

IChC current density contains components of the carrier drift (n_{tr}) (due to separation of electrons and holes by the external dc electric field during initial instants of the photo-excitation by short laser pulse), and the ambipolar diffusion of the quasi-neutral domain of excess carriers ($n_{R\text{-}D} \approx p_{R\text{-}D}$), after this electric field is screened. As a measure for re-distribution within carrier densities decay through carrier diffusion-recombination ($n_{D\text{-}R}$) and drift (n_{tr}) can be a threshold value of charge (q) affordable to shift by applied external voltage. Charge q can be evaluated by utilizing the system capacitance (C) and the relation $q=CU$. Carrier density involved into charge transit is evaluated by using an approximation of parallel-plate capacitor of an area S, and is expressed as

$$n_{tr}=CU/eSd^* = \varepsilon\varepsilon_0 U/e\Delta d^*. \tag{5}$$

Here, d^* denotes the capacitor effective width, and Δ is an excess carrier domain width. Actually, this n_{tr} is limited by the diode geometrical capacitance ($d^* \leq d$) and by the external voltage U.

Actually, at rather low voltages and large excitation densities, the external electric field E_0 is rapidly screened within distances of $L_E=eE_0L_D^2/k_BT$ due to decrease of the Debye radius $L_D=(\varepsilon\varepsilon_0 k_BT/2e^2n_{ex})^{1/2}$ varied with enhancement of excess carriers of density n_{ex}. Then the diffusion field $E_D=k_BT/eL_D$ prevails for $L_E/L_D<<1$. Screening appears during a dielectric relaxation $\tau_M=\varepsilon\varepsilon_0/e\mu n_{ex}$ or a drift $\tau_{tr}= d^{*2}/\mu U$ time for carriers of mobility μ if τ_M, $\tau_{tr} << \tau_R$ owing to initially generated excess carriers n_{ex0}, and n_{tr} vanishes ($n_{tr} \to 0$) within initial transient stages when n_{ex} is large. Then, the light induced domain of excess carriers is able to dissipate through electrodes due to diffusion across the base and carrier extraction by electric field at p^+n and nn^+ junctions. The simplified approximation of carrier domain drift and diffusion process can be described by a classical expression[17] for carrier density variations dependent on time and position as:

$$n_{R-D}(x,t) = (n_{ex0} - n_{tr}(t))\frac{d^*}{\sqrt{4\pi D_A t}} \exp(-\frac{t}{\tau_R}) \exp[-\frac{(x-\mu Et)^2}{4D_A t}]. \tag{6}$$

Here, n_{ex0} is an initial (t=0) density of bipolary photo-excited carriers, D_A is a coefficient of carrier ambipolar diffusion. Due to probing regime (either IChCC or MW-PC-E), a signal is sensitive either to carrier density at collecting electrode ($n_{R\text{-}D}(t,d)$) for IChCC or depth integrated carrier density $(1/d)\int_0^d n_{R\text{-}D}(t,x)dx$ for MW-PC-E response, respectively. In the latter case, the time dependent variations of depth averaged carrier density registered by MW-PC-E can be expressed as:

$$< n_{MW-PC-E}(t) >_d = (n_{ex0} - n_{tr}(t)) \exp(-\frac{t}{\tau_R})\{erf[\frac{d}{\sqrt{4D_A t}} - \frac{\mu_A E\sqrt{t}}{\sqrt{4D_A}}] + erf[\frac{\mu_A E\sqrt{t}}{\sqrt{4D_A}}]\}. \tag{7}$$

The specific fast changes (caused by small charge drift or flight, by extraction of charge reservoir prior complete external field screening is reached) are ignored within measured vertex of MW-PC-E pulse. Hereby, the MW-PC-E transient appears to be a trapezium-like pulse with relaxation of a vertex descending component. A slope of the latter constituent is varied by recombination lifetime.

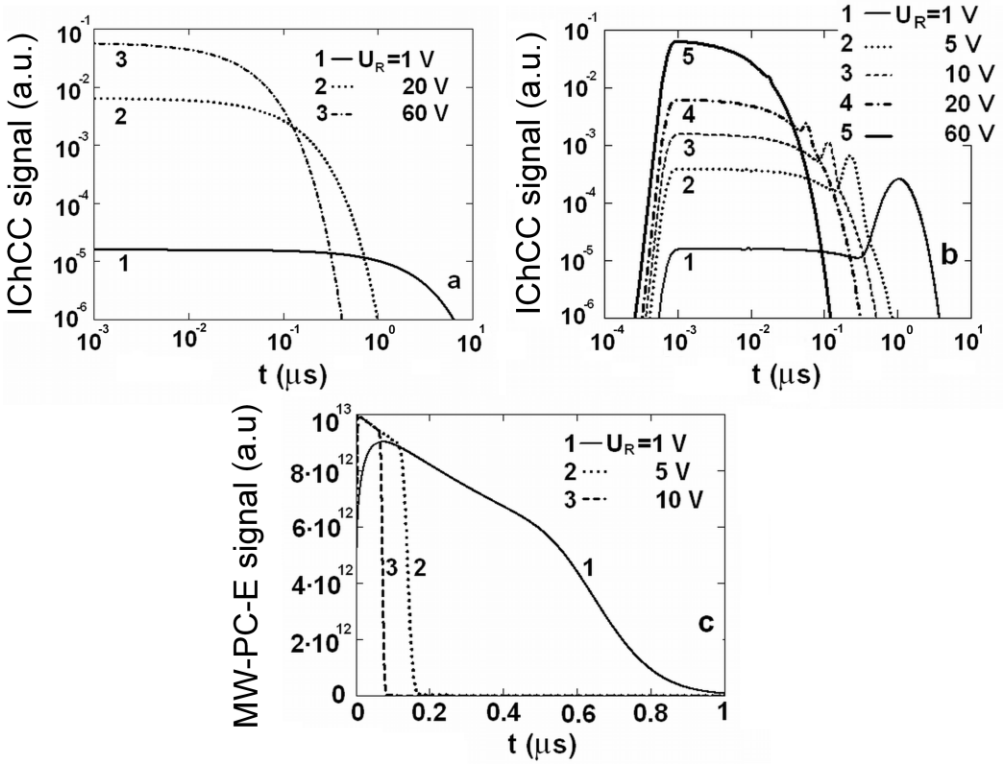

FIG. 7. Simulated induced bulk charge collection current (IChCC) transients: a - for condition $n_{R\text{-}D}(t,d) < n_{tr}(t)$, and b- for initial condition $n_{R\text{-}D}(t,d) > n_{tr}(t)$ which varies as a function of applied voltage. c- Simulated MW-PC-E transients at different applied reverse voltages U.

This slope of a trapezium-like pulse can be used for extraction of the recombination lifetime value. On the other hand, duration of vertex plateau, within MW-PC-E transient, indicates a diffusion time of the pulsed excited carrier domain.

The transient shape, dependent on the ratio of $n_{R\text{-}D}(t,d)/n_{tr}(t)$, changes with enhancement of excitation density. At a rather small excitation density (close to values for registration of the ICDC response), IChCC transient is inherent for a relaxation process with characteristic lifetime of $\tau_{Reff} = 1/(\tau_{capt}^{-1}+\tau_R^{-1})$ on the pulse vertex. However, at a rather high surface excitation density with $n_{R\text{-}D}(t,d)/n_{tr}(t)>1$, IChC current acquires a rising rearward peak pulse, which amplitude at initial instants is close to zero. Duration of such a pulse is close to $\tau_D \cong d^2/4\pi^2 D_A$. For a fixed applied voltage U, the changes of the IChCC transient shape are governed through a ratio of $n_{R\text{-}D}(t,d)/n_{tr}(t)$ via an initially light induced excess carrier density, and it is approximated by using equations (5)–(7). The ICDC component can be also observed as a hog on the rising initial step of the IChCC transient pulse if the initial transient stage is displayed on a proper temporal scale. The aforementioned peculiarities in the simulated IChCC characteristic transients are illustrated in FIG. 7.

Peculiarities in extracting carrier recombination and trapping parameters from the MW-PC transients measured in wafer samples without applied electric field are mentioned in 7. The applied electric field acts in parallel with the carrier recombination processes in disappearance of the excess carries from the diode base region. Therefore, duration of the MW-PC-E transient registered under bias field (E) depends on the applied voltage (U). Then, a transient contains an inherent slope within rearward component of the MW-PC-E pulse (inset of FIG. 1) indicating that the final stage of the carrier disappearance from the diode base region is governed by the prevailing charge drift processes caused by the applied electric field (within time segments when densities of excess carriers are sufficiently reduced). The fast rearward component of the MW-PC-E pulse coincides in time (inset of FIG.1) with induced charge collection (IChCC) peak. To obtain a MW-PC signal it is necessary

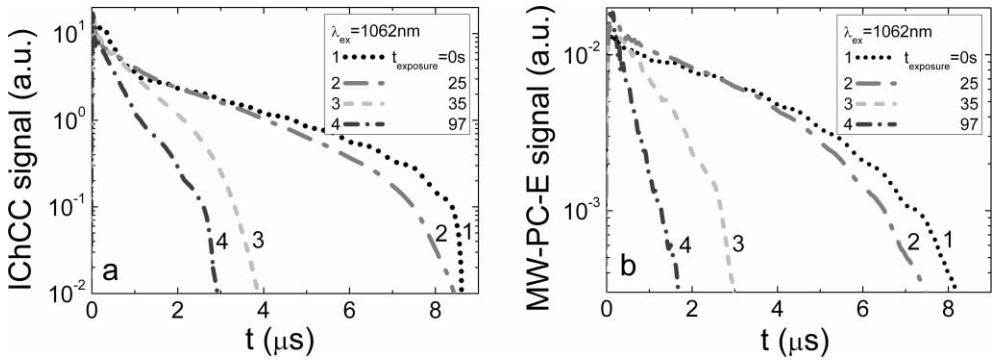

FIG. 8. Variations of the IChCC (a) and MW-PC-E (b) transients registered in situ during 8 MeV proton irradiation of a Si pad-detector when the bulk excitation density and applied bias voltage $U \cong U_{FD}$ were fixed.

to excite the elevated excess carrier densities compared to those in detection of the ICDC signal due to the difference in the sensitivities of the MW and electrical contact probes.

Based on the above discussed modeling, variations of the experimental transients, illustrated in FIG. 6, can be interpreted as follows: a- for the regime of bulk excitation, IChCC transients exhibit a smoothed double peak shape, while ulterior stage of the transient is delayed by carrier capture/multi-trapping processes; b- for surface excitation regime using moderate excess carrier densities, excess carrier diffusion determines duration of the vertex component within a trapezoidal IChCC pulse. A slope of this vertex descending component indicates the recombination duration. Drift of carriers manifests only within the ulterior, a rapidly decreasing constituent of the IChCC current pulse. Increment of applied voltage above values of full depletion (U_{FD}) enhances density of carrier (n_{tr}) governed by applied field. Then IChCC pulses are shortened and acquire a double peak shape (as for ICDC transients) due to a reduction of the ratio $n_{R\text{-}D}(t,d)/n_{tr}(t) << 1$ in accordance to applied voltage magnitude; c- for a reverse voltage below U_{FD} and in the range of large surface excitation densities, enhancement of excess carrier density leads to a prevailing diffusion of the excess carrier domain, with $\tau_D = d^2/\pi^2 D_A$. Then the IChCC pulse stretches with increment of n_{ex}, as the time, necessary to completely extract the light injected carriers, is increased.

Carrier decay times and carrier diffusion coefficient values estimated from the IChCC transients are in agreement with the parameters measured by MW-PC and ICDC techniques.

2. Evolution of transients during irradiation

The correlated evolution of IChCC (a) and MW-PC-E (b) transients, registered simultaneously during 8 MeV proton irradiation and using fixed excitation density and voltage, are illustrated in FIG. 8.

The correlated decrease of both IChCC and MW-PC-E pulse duration as a function of irradiation time can be easily noted even for short exposure times. A slope within a vertex of the trapezoidal–like IChCC transients (sketched within FIG. 8(a)) is employed for extraction of carrier lifetime. While, the faster slope within backward component of a transient is exploited for evaluation of carrier transit time. Similarly in FIG. 8(b), a slope of within vertex component of the trapezoidal–like MW-PC-E transient is used for evaluation of effective carrier diffusion-recombination lifetime, and a slope of the ulterior constituent in MW-PC-E transient shows a rate of carrier extraction by applied field.

Values of the reciprocal characteristic times are plotted in FIG. 9 vs. proton irradiation exposure time. Actually, the latter exposure time indicates the irradiation fluence, estimated within the upper scale. It can be deduced from FIG. 9, that the reciprocal recombination (FIG.5) lifetime increases with exposure time (irradiation fluence is assumed to be proportional to exposure time) near linearly during initial irradiation stages. However, at elevated fluences, values of the effective recombination lifetime τ_R measured by the MW-PC-E technique on diodes with applied electric field start to saturate. This can be easily understood by manifestation of multi-trapping effect, when several centers (recombination and trapping) act together, due to effective generation of point defects

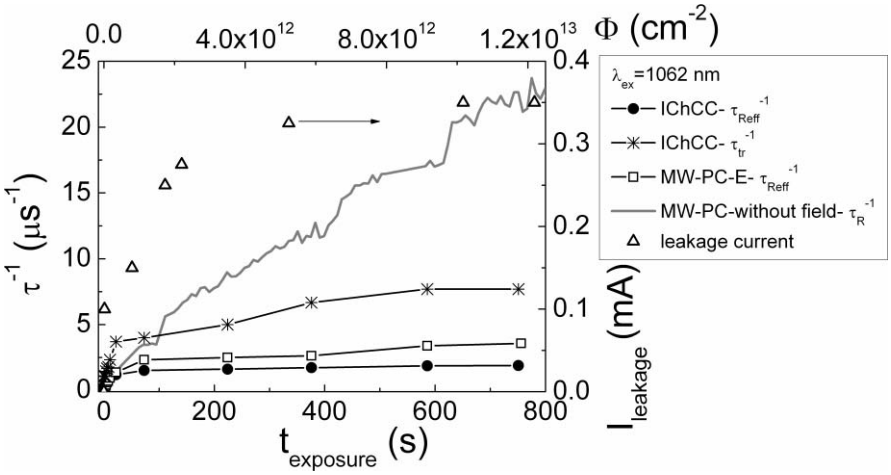

FIG. 9. Irradiation exposure (∼ fluence) dependent the reciprocal values of the excess carrier recombination lifetime evaluated by MW-PC transients without applied electric field (grey curve) and of effective recombination (solid circles and open squares) and of drift (stars) times extracted from IChCC (solid circles) as well as from MW-PC-E (open squares), respectively, using transients registered in situ during 8 MeV proton irradiation of a Si pad-detector when the excitation density and applied bias voltage $U \cong U_{FD}$ were fixed.

during irradiation by protons. Saturation of the effective recombination lifetime (which averages the carrier recombination and multi-trapping rate) correlates well with enhancement of leakage current relatively to the irradiation exposure time scale. The charge collection is delayed if carrier trapping increases. The latter can be also increased due to reduction of carriers within a neutral diode region, i.e. if Debye length outspreads and dielectric relaxation time lengthens. Complementarily, values of reciprocal transit time are saturated within a range of elevated exposures (equivalent to $>6\times 10^{12}$ cm^{-2}).

The range of saturation for τ_{tr} coincides with region of saturated of effective carrier recombination lifetime τ_{Reff} values (when evaluation is performed using IChCC transients) and with that of generation current, proportional to a leakage current simultaneously measured and also presented in FIG. 9. This result indicates that a reduction of τ_{Reff} is correlated well with enhancement of τ_{tr}. Such a correlation can be understood if carrier capture rate ($\sim 1/\tau_{Reff}$) modifies the dielectric relaxation within evolution of IChCC transients. It can be noticed in FIG. 9 for τ_{tr} values extracted form MW-PC-E, that impact of applied field is important (τ_{tr} can be evaluated), only in the range of rather small fluences. For the enhanced irradiation exposure times, precision of τ_{tr} separation, within MW-PC-E transient, falls down, and these values follows the fluence dependent variation of τ_{Reff}. Reasons are the same, - interplay of carrier recombination and multi-trapping and of transit processes is enhanced with fluence, when material approaches to insulating state, and resolution for extraction of τ_{Reff} and τ_{tr} decreases when applying IChCC and MW-PC-E techniques. For comparison, evolution of carrier recombination lifetime, evaluated by in situ carrier lifetime measurements for wafer samples by the MW-PC technique[7] without applied voltage, keeping the same other experimental conditions, is also shown in FIG. 9. The latter curve exhibits clear increase of τ_R^{-1}(when multi-trapping effects are suppressed) with irradiation exposure time, while τ_R values are in good agreement with those measured by IChCC and MW-PC-E in several segments of exposure characteristic.

V. SUMMARY

A multi-functional instrument and techniques suitable for simultaneous monitoring of the evolution of radiation defects and of changing of functional characteristics of Si particle detectors during irradiation with protons are described. The employed techniques are based on microwave probed variations of carrier recombination parameters at the applied electric field. The currents caused by charge collection due to carrier drift-diffusion flows in the Si detector structures are measured as

well. The leakage current variations are also remotely controlled. The components of this instrument have been designed and fabricated at Vilnius University and installed at accelerator facilities of the Department of Physics, Division of Materials Physics, Helsinki University. The techniques have been tested by varying and combining various measurement regimes. Tentative experiments showed a proper sensitivity of the instruments and techniques for monitoring of defect creation and their competition during irradiations with different energy protons and an evolution of defects during proton beam action. The interplay of carrier recombination and transport processes is enhanced with fluence, when material approaches to insulating state, and resolution for extraction of τ_{Reff} and τ_{tr} decreases when applying IChCC and MW-PC-E techniques.

ACKNOWLEDGEMENTS

Authors appreciate J. Harkonen and E. Tuominen for provided Si pad-detectors. J. Kaladė is acknowledged for fruitful discussions and recommendations in analysis of the theoretical aspects of carrier transport. A.Uleckas is acknowledged for design of software for IChCC instrument and help in measurements. This work has been performed in frame of the CERN-RD39 collaboration. The financial support of the Academy of Finland (Project No. 132128) is gratefully acknowledged.

[1] I. Pintilie, E. Fretwurst, G. Lindstroem, and J. Stahl, Appl. Phys. Lett. **82**, 2169 (2003).
[2] M. Mikelsen, J. H. Bleka, J. S. Christensen, E. V. Monakhov, B. G. Svensson, J. Harkonen, and B. Avset, Phys. Rev. B **75**, 155202 (2007).
[3] M. Scaringella, D. Menichelli, A. Candelori, R. Rando, and M. Bruzzi, IEEE Trans. Nucl. Sci, **53**, 589 (2006).
[4] V. Eremin, N. Strokan, E. Verbitskaya, and Z. Li, Nucl. Instrum. Meth. Phys. Res. A **372**, 388 (1996).
[5] J. Härkönen, V. Eremin, E. Verbitskaya, S. Czellar, P. Pusa, Z. Li, and T. O. Niinikoski, Nucl. Instrum. Meth. Phys. Res. A **581**, 347 (2007).
[6] M. Huhtinen, Nucl. Instrum. Meth. Phys. Res. A **491**, 194 (2002).
[7] E. Gaubas, A. Uleckas, J. Vaitkus, J. Raisanen, and P. Tikkanen, Review Sci. Instrum. **81**, 053303 (2010).
[8] S. Väyrynen, P. Tikkanen, J. Räisänen, I. Kassamakov, and E. Tuominen, J. Appl. Phys. **106**, 024908 (2009).
[9] H. Amekura, N. Kishimoto, and K. Kono, Journ. Appl. Phys. **84**, 4834 (1998).
[10] www.cern.ch/rd50.
[11] S. Väyrynen, J. Räisänen, I. Kassamakov, and E. Tuominen, J. Appl. Phys. **106**, 104914 (2009).
[12] P. Blood and J. W. Orton, *The electrical characterization of semiconductors: majority carriers and electron states* (Academic Press, London –San Diego-New York, 1992).
[13] B. Y. Baliga. *Power semiconductor devices*, (PWS Publishing Company, Boston, 1995).
[14] M. A. Lampert, P. Mark, *Current injection in solids*, (Acad., New York, 1970).
[15] C. Leroy, P. Roy, G. Casse, M. Glaser, E. Grigoriev, F. Lemeilleur, Nucl. Insrum. Meth. Phys. Res. A **426**, 99 (1999).
[16] E. Gaubas, A. Uleckas, and J. Vaitkus, Nucl. Instr. Methods in Phys. Res. A **607**, 92 (2009).
[17] R. Smith, *Semiconductors*, 2nd edn. (Cambridge Univ. Press, London - New York, 1982).